

# Numerical Simulation of the Navier–Stokes Equations Using the Artificial Compressibility (AC) Method with the 4th Order Artificial Dissipation Terms

Kidoo Park\*, Kil Seong Lee\*\*

.....

## Abstract

The artificial compressibility (AC) method for the incompressible Navier–Stokes equations in the generalized curvilinear coordinates using the primitive form is implemented. The main advantage of the AC approach is that the resulting system of equations resembles the system of compressible N–S equations and can thus be integrated in time using standard, well-established time-marching methods. The errors, which are the odd–even oscillation, for pressure field in using the artificial compressibility can be eliminated by using the 4<sup>th</sup> order artificial dissipation term which is explicitly included. Even though this paper focuses exclusively on 2D laminar flows to validate and assess the performance of this solver, this numerical method is general enough so that it can be readily extended to carry out 3D URANS simulation of engineering flows. This algorithm yields practically identical velocity profiles and primary vortex and secondary vortices that are in excellent overall agreement with the results of the vorticity–stream function formulation (Ghia et al., 1982). However, the grid resolution have to be required to be large enough to express the various vortices.

*Keywords:* Navier–Stokes Equations, Generalized Curvilinear Coordinates, Artificial Compressibility Method, Odd–even Oscillation, Artificial Dissipation Terms, URANS simulation, Primary Vortex, Secondary Vortices, Vorticity–Stream Function, Grid Resolution

.....

## 1. Introduction

Almost numerical errors that appear in the literatures (Ferziger et al., 1994; Figitas et al., 1993) are associated with the discretized convective terms in motion even if turbulence modeling is not included. The numerical method needs to introduce the artificial dissipation terms (Rogers et al., 1990; Rogers et al., 1991) in order to eliminate the numerical errors. I will deal with solving incompressible Navier–Stokes equations using the primitive form which is artificial compressibility (AC) method. The main advantage of the AC approach is that the resulting system of equations resembles the system of compressible N–S equations and can thus be integrated in time using standard, well-established time-marching methods. The errors, which are the odd–even oscillation, for pressure field in using AC method can be eliminated by using the 4<sup>th</sup> order artificial dissipation term which is explicitly included.

---

\* Ph. D. student, Department of Civil and Environmental Engineering, Seoul National University · E-mail : hydrol88@snu.ac.kr

\*\* Professor, Department of Civil and Environmental Engineering, Seoul National University · E-mail : kilselee@snu.ac.kr

Therefore, this numerical study with the artificial dissipation terms is employed and the multigrid method is also implemented. Multigrid method applies an iterative scheme in this study since the total amount of computational effort does not significantly increase even though the method converges faster (Ghia et al., 1982; Tang et al., 2003).

## 2. Governing Equations

Using the generalized coordinate transformations, along with the formulas for transforming the various differential operators, the Navier-Stokes equations can be formulated in generalized curvilinear coordinates as follows:

$$\frac{1}{J}\Gamma\frac{\partial\mathbf{Q}}{\partial t}+\frac{\partial\tilde{\mathbf{E}}}{\partial\xi}+\frac{\partial\tilde{\mathbf{F}}}{\partial\eta}-\frac{\partial\tilde{\mathbf{E}}_v}{\partial\xi}-\frac{\partial\tilde{\mathbf{F}}_v}{\partial\eta}=\mathbf{0}$$

where

$$\tilde{\mathbf{E}}=\frac{1}{J}(\xi_x\mathbf{E}+\xi_y\mathbf{F}) \quad , \quad \tilde{\mathbf{F}}=\frac{1}{J}(\eta_x\mathbf{E}+\eta_y\mathbf{F}) \quad , \quad \tilde{\mathbf{E}}_v=\frac{1}{J}(\xi_x\mathbf{E}_v+\xi_y\mathbf{F}_v) \quad , \quad \tilde{\mathbf{F}}_v=\frac{1}{J}(\eta_x\mathbf{E}_v+\eta_y\mathbf{F}_v) \quad .$$

The governing equation is as follows:

$$\Gamma = \text{diag}(0, 1, 1) \quad , \quad \mathbf{Q} = [p, u, v, w]^T$$

$$\tilde{\mathbf{E}} = \frac{1}{J} \begin{bmatrix} U \\ uU + \frac{1}{\rho}P\xi_x \\ vU + \frac{1}{\rho}P\xi_y \end{bmatrix} \quad , \quad \tilde{\mathbf{F}} = \frac{1}{J} \begin{bmatrix} V \\ uV + \frac{1}{\rho}P\eta_x \\ vV + \frac{1}{\rho}P\eta_y \end{bmatrix} \quad ,$$

$$\tilde{\mathbf{E}}_v = \frac{1}{J Re} \begin{bmatrix} 0 \\ g^{11}\frac{\partial u}{\partial\xi} + g^{12}\frac{\partial u}{\partial\eta} \\ g^{11}\frac{\partial v}{\partial\xi} + g^{12}\frac{\partial v}{\partial\eta} \end{bmatrix} \quad , \quad \tilde{\mathbf{F}}_v = \frac{1}{J Re} \begin{bmatrix} 0 \\ g^{12}\frac{\partial u}{\partial\xi} + g^{22}\frac{\partial u}{\partial\eta} \\ g^{12}\frac{\partial v}{\partial\xi} + g^{22}\frac{\partial v}{\partial\eta} \end{bmatrix} \quad .$$

where  $\{g^{ij}\}$  is the so-called contravariant metric tensor,

$$\{g^{ij}\} = \{g^i \cdot g^j\} = \begin{bmatrix} g^{11} & g^{12} \\ g^{12} & g^{22} \end{bmatrix} = \begin{bmatrix} \xi_x^2 + \xi_y^2 & \xi_x\eta_x + \xi_y\eta_y \\ \xi_x\eta_x + \xi_y\eta_y & \eta_x^2 + \eta_y^2 \end{bmatrix} \quad ,$$

and the covariant velocity components as follows:

$$U = V^1 = \mathbf{V} \cdot \mathbf{g}^1 = u \frac{\partial\xi}{\partial x} + v \frac{\partial\xi}{\partial y}$$

$$V = V^2 = \mathbf{V} \cdot \mathbf{g}^2 = u \frac{\partial\eta}{\partial x} + v \frac{\partial\eta}{\partial y} \quad .$$

$Re$  is the Reynolds number of the flow.

### 3. Numerical Methods

The governing equations in generalized curvilinear coordinates, using dual or pseudo time-stepping Artificial Compressibility (AC) method to couple pressure and velocities, are the three-dimensional, incompressible Navier–Stokes (NS) equations and continuity equation, nondimensionlized by  $\rho$ ,  $U_o$ , and  $L_o$ . The governing equations follow

$$\begin{aligned}\Gamma \frac{\partial Q}{\partial t} + J \frac{\partial}{\partial t} (F^l - F_\nu^l) &= 0, \\ \Gamma &= \text{diag}(0, 1, 1), \\ Q &= (P, u_1, u_2)^T, \\ F^l &= \frac{1}{J} (U^l, u_1 U^l + P \xi_{x_1}^l, u_2 U^l + P \xi_{x_2}^l), \\ F_\nu^l &= \frac{1}{J Re} \left( 0, g^{ml} \frac{\partial u_1}{\partial \xi^m}, g^{ml} \frac{\partial u_2}{\partial \xi^m} \right)^T,\end{aligned}$$

where  $x_l$  are the Cartesian coordinates  $x$ ,  $y$ , and  $z$ .  $\xi^l$  are curvilinear coordinates  $\xi$ ,  $\eta$ , and  $\zeta$ , respectively,  $\xi_{x_m}^l$  are the metrics of the geometric transformation,  $g^{ml}$  are the components of the contravariant metric tensor, and  $J$  is the Jacobian of the geometric transformation.  $U^l$  are the contravariant velocity components,  $U^l = u_m \xi_{x_l}^m$ ,  $u_m$  are the Cartesian velocity components,  $u$  and  $v$ , and  $P$  is the static pressure divided by the density. Finally,  $Re$  is the Reynolds number of the flow, which is based on characteristic length and velocity scales and the kinematic viscosity of the fluid.

The governing equations are discretized in strong conservation form using a three-point backward, second-order accurate Euler implicit scheme for the temporal derivative and three-point, second order accurate central differencing for the spatial derivatives,

$$\Gamma \frac{1}{J} \left( \frac{dQ}{dt} \right)_{i,j} + (\delta_{\xi^l} \tilde{F}^l + \delta_{\xi^l} \tilde{F}_\nu^l)_{i,j}^{n+1} = 0$$

where  $\delta_{\xi^l}(\cdot)_{i,j} = \frac{(\cdot)_{i+1/2,j} - (\cdot)_{i-1/2,j}}{\Delta \xi^l}$ .

The flux  $\tilde{F}$  is the flux  $F$  at the cell interfaces and  $D$  is the artificial dissipation flux, especially, the matrix-valued scheme (Lin and Sotiropoulos, 1997),

$$\begin{aligned}\tilde{F}_{i+1/2,j}^1 &= \frac{1}{2} (F_{i,j}^1 + F_{i+1,j}^1) + D_{i+1/2,j}^1 \\ D_{i+1/2,j}^1 &= \epsilon \delta_{\xi^l} (|A| \delta_{\xi^l} \delta_{\xi^l}) Q_{i+1/2,j}\end{aligned}$$

where  $\epsilon$  is a constant,  $|A^l|$  is the absolute value of the Jacobian matrix  $A^l = \partial F^l / \partial Q$ .

The efficiency and robustness of the algorithm can be enhanced by implementing the local dual-time-stepping. A pseudo-time derivative term is added to the discrete governing equations until the pseudo-time derivative is reduced to a small residual and the time accurate N-S equations are satisfied at the next physical time step.

$$Q_{i,j}^{n+1,m} = Q_{i,j}^{n+1,0} - \alpha_m \Delta \tau \left[ \Gamma \frac{3 Q_{i,j}^{n+1,m-1} - 4 Q_{i,j}^n + Q_{i,j}^{n-1}}{2 \Delta t} + J(\delta_{\xi^1} \tilde{F}^l + \delta_{\xi^1} \tilde{F}^l)_{i,j}^{n+1,m-1} \right]$$

where  $\Delta \tau$  is the pseudo-time step increment,  $\alpha_m$  are the Runge-Kutta coefficients ( $= 1/m$ , for  $m = 1, 2, 3, 4$ ). Thus,  $Q$  terms at the pseudo-time level is treated as  $Q^{n+1,0} = [Q^{n+1}]^\tau$ ,  $Q^{n+1,4} = [Q^{n+1}]^{\tau + \Delta \tau}$ .

The local time step is computed

$$\Delta \tau = \frac{CFL}{\max(\lambda_{\xi^1}, \lambda_{\xi^2})}$$

where  $\lambda_{\xi}$  is the spectral radii of the Jacobian matrices,  $CFL$  is the Courant-Friedrich-Lewis number.

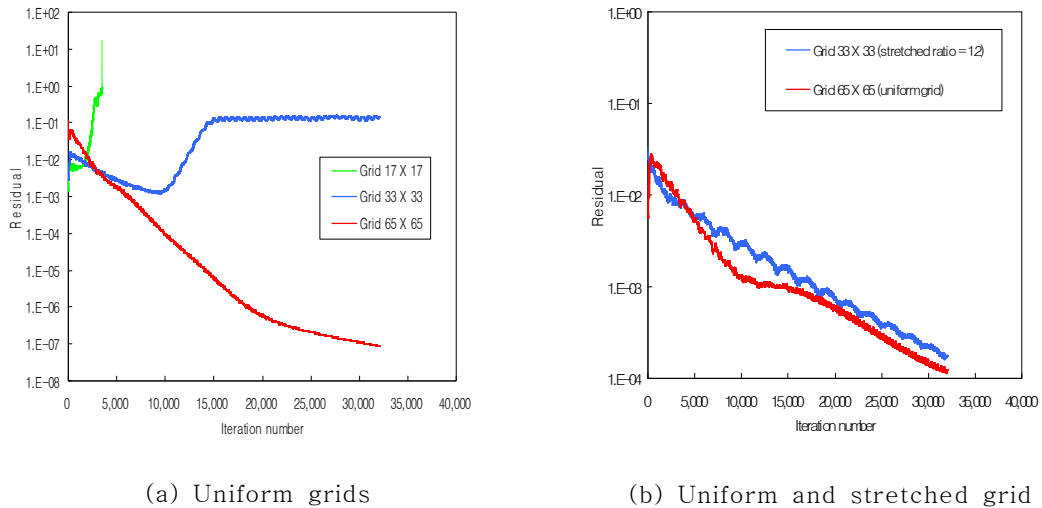
#### 4. Numerical Experiment

This solver was used to evaluate and compare this computed results with the benchmark solutions of Ghia et al. (1982) for steady, laminar flow in a square driven cavity whose upper wall is moving at constant speed  $u = 1.0$  using both uniform and stretched grids. No slip and no flux boundary conditions, implemented by Dirichlet conditions, at the nonporous walls yields that every velocity is zero at all the boundaries except at the moving wall. The pressure at all boundaries is obtained by the linear extrapolation from interior nodes.

For the cavity flow,  $17 \times 17$ ,  $33 \times 33$ , and  $65 \times 65$  grid nodes with uniform meshes are used to investigate the grid sensitivity of the grid. To investigate the effects of the computational efficiency, I made a use of both  $65 \times 65$  grid nodes with uniform meshes and  $33 \times 33$  grid nodes of stretched mesh whose grid stretched ratio is 1.2. The minimum near-walls grid spacing is 0.001 and the maximum grid stretching ratio is 1.35 (Lin and Sotiropoulos, 1997). The  $CFL$  number for all the simulations is  $CFL = 0.5$  to eliminate the difference of the computational efficiency and the pseudo-compressibility parameter is set to  $\beta = 1$ . In the all two directions, the artificial dissipation parameter  $\epsilon$  is set equal to 0.01.

#### 5. Results and Conclusion

The numerical study is carried to do the grid refinement study according to the convergence properties and computational efficiency. At especially,  $Re = 1000$ , using the inadequacy of coarse meshes (less than  $65 \times 65$ , meshes), the solution is not converged and it blow up as shown in Figure 1. Therefore, because the result of a driven cavity flow at high  $Re$  at very coarser grid cannot provide better results than that of a fine-grid solution for high  $Re$  flow.

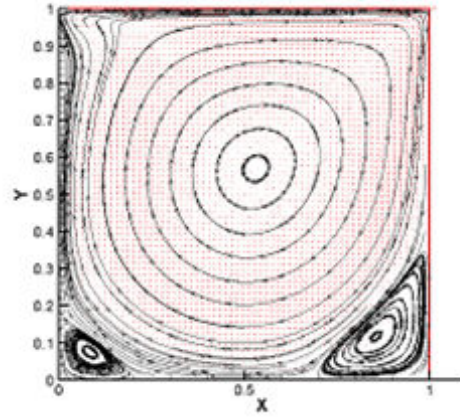


(a) Uniform grids (b) Uniform and stretched grid  
**Figure 1. Convergence histories for uniform and stretched grid ( $Re = 1,000$ )**

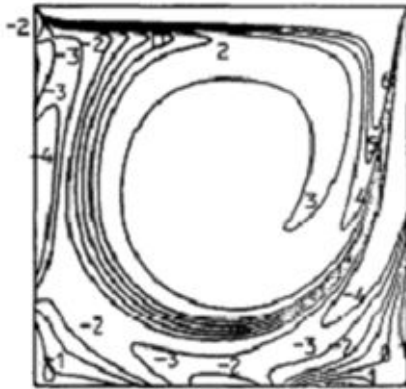
As shown in Figure 2, two secondary vortex at the both bottom corners in  $65 \times 65$  nodes are expressed, when present results are compared with Ghia's results of streamline and vorticity. However, any secondary vortex dose not appear at the right and left bottom corner in  $17 \times 17$  nodes. As shown in Figure 3, these of stretched meshes with stretching ratio 1.2 yield a practically identical streamlines and velocity profiles compared with these of the uniform meshes. The secondary vorticity and also primary vortex are computed very well in the stretched meshes. Vorticity contours except the center of primary vortex make a good agreement in Figure 3.



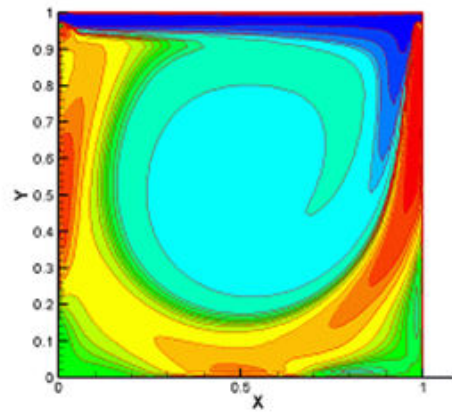
(a) Ghia et al., 1982 ( $129 \times 129$ )



(b) Present result ( $65 \times 65$ )

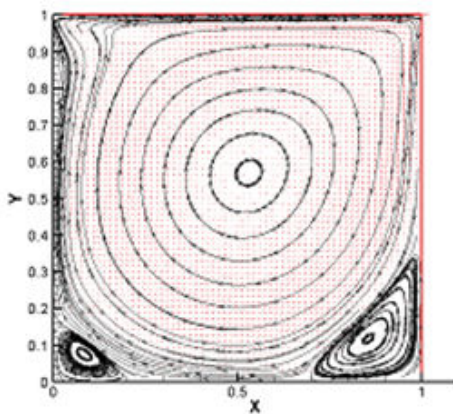


(c) Ghia et al., 1982 ( $129 \times 129$ )

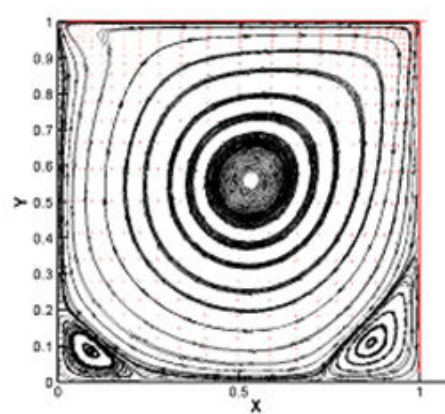


(d) Present result ( $65 \times 65$ )

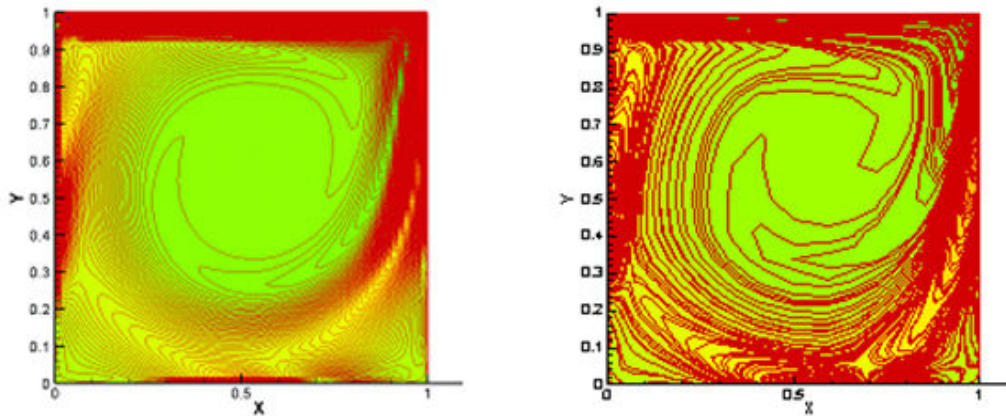
**Figure 2. streamline and vorticity contour for uniform mesh ( $Re = 1,000$ )**



(a) Uniform meshes ( $65 \times 65$ )



(b) Stretched meshes ( $35 \times 35$ )



(c) Uniform meshes ( $65 \times 65$ )

(d) Stretched meshes ( $35 \times 35$ )

**Figure 3. streamline and vorticity contour of driven cavity ( $Re = 1,000$ )**

I found that computational efficiency is a combination of convergence speed and a given grid size through the grid refinement study. If high computational efficiency will be required at the less CPU time as to reduce the total mesh size, I suggest that stretched grids should be used to save CPU time. However the use of too coarser meshes makes the spoilage of numerical results. In conclusion, the computational solution using coarser meshes with stretched grids is alternative to save the total CPU time which is compared with that of the finer meshes. Even if we choose stretched coarser grids of the same size of which it is impossible to get a numerical solution for uniform grid, the effect of the grid resolution should be reduced as to compressing the grids near the wall because the difference of velocity gradient between grids could be reduced near the wall.

### Acknowledgement

The authors wish to acknowledge the financial support by SNU SIR Group of the BK21 research Program funded by Ministry of Education & Human Resources Development.

### References

1. Ferziger, J. H. (1994). "Comments on the policy statement on numerical accuracy." *ASME J. of Fluids Eng.*, Vol.116, p.396.
2. Freitas, C. J. (1993). "Editorial policy statement on the control of numerical accuracy." *ASME J. of Fluids Eng.*, Vol.115, p.339.
3. Ghia, K. N., Ghia, and Shin, C. T. (1982). "High- $Re$  Solutions for incompressible flow using the Navier-Stokes equations and a multigrid method." *J. of Comp. Physics*, Vol.48, pp.387-411.
4. Lin, F. B., and Sotiropoulos, F. (1997). "Assessment of artificial dissipation models for

- three-dimensional incompressible flow solutions." *ASME J. Fluids Eng.*, 119(2), pp.331-340.
5. Rogers, S. E., and Kwak, D. (1990). "Upwind differencing schemes for the time-accurate incompressible Navier-Stokes equations." *AIAA Journal*, Vol.28, No.2, pp.253-262.
  6. Rogers, S. E., Kwak, D., and Kiris, C. (1991). "Steady and unsteady solutions of the incompressible Navier-Stokes equations." *AIAA Journal*, Vol.29, No.4, pp.603-610.
  7. Rubin, S. G., and Graves, R., A., Jr. (1975). "Cubic spline solution for the driven cavity problem." *NASA SP-378*.
  8. Tang, H. S., Jones, S. C., Sotiropoulos, F. (2003). "An overset-grid method for 3D unsteady incompressible flows." *J. Comp. Phys.* Vol.191, pp.567-600.